Sana'a University Journal of Applied Sciences and Technology

Vol. 1 | No. 1 | Page 83 – 92 | 2023| https://jpurnals.su.edu.ye/jast

Modulated ion-acoustic wavepackets in a multi-component dense plasma with Thomas-Fermi distribution

Mahmood Ahmed. Hassan. Khaled[1,*]; Mohmed Ali. Shukri[1]; Rowaida A. A. Fare'e[2],

[1]Department of Physics, Faculty of Science, Sana'a University, Sana'a, Yemen
[2]Department of Physics, Faculty of Education, Sana'a University, Sana'a, Yemen
*Corresponding author: Mahmood A. H. Khaled; Email:mahkhaled@hotmail.com

ARTICLE INFO
Article history:
Received: December 24, 2022
Accepted: January 17, 2023
Published: January, 2023

Keywords
1. Wavepackets
2. Envelop solitons
3. Nonlinear Schrödinger equation
4. Modulational instability

ABSTRACT: Modulated ion acoustic wavepackets have been investigated in a multi-component, dense plasma containing degenerate electrons/positrons, and positive/negative ions. It is assumed that both electrons and positrons follow the Thomas-Fermi statistic, while the positive and negative ions are considered to be classic. Using a multiscale perturbation method, the nonlinear Schrödinger equation is derived. The modulational instability conditions have been analyzed for modulated ion acoustic waves. The influences of dense plasma parameters on the modulational instability and its growth rate have been discussed. The envelope solitons have been discussed as well. The results showed that both modulationally unstable domain and stable domain can be found, depending on the plasma parameters. It was also found that the width of the envelop solitons is significantly affected by the relevant dense plasma parameters. The present results may be useful in understanding the instability criteria of modulated ion acoustic waves which are related to both space and laboratory dense plasmas.

CONTENTS

1. Introduction

Dense plasma is a type of plasmas characterized by very low thermal temperature and very high number density of particles. It can be found in astrophysical objects, like white dwarf [1], neutron stars [1, 2] and under laboratory conditions in laser fusion [3], ultra-small electronic devices [4] and micro-pinch experiments [5]. At very dense plasmas, the thermal de-Broglie's wavelength of plasma particles can be compared to interparticle distance [6, 7]. Thus, the thermal energy of these particles becomes much less than the Fermi's energy, which means that their thermal pressure can be ignored compared to the Fermi's pressure. In such a dense plasma the particles become degenerate and the classical statistics are inappropriate to describe their behavior. In fact, the quantum Thomas–Fermi statistic may be suitable for describing the dynamic behavior of these particles [8]. Over the last few years, the dynamics of linear/nonlinear electrostatic acoustic mode in a dense plasma become one of the major research areas in plasma physics because of its major role in understanding not only astrophysical environments but also laboratory devices [1-5]. Dubinov and Dubinova [9] have investigated the ion acoustic waves (IAWs) in an ideal plasma its components are classical ions and degenerated electrons. The propagation of arbitrary amplitude IAWs in a dense electron-positron-ion plasma are investigated by Abdelsalam et al. [10]. They considered that electrons and positrons are described by Thomas-Fermi statistics. Further, by considering Thomas-Fermi distribution of electrons

and positrons, Mehdipoor and Esfandyari-Kalejahi [11] have investigated the nonlinear propagation of small amplitude IAWs in a dense plasma containing classical warm ions fluid and degenerate positrons-electrons.

On the other side, due to the nonlinearity of the plasma medium, the nonlinear wave in such plasma may be subject to amplitude modulation [12] and the result is modulated wave packets propagating in such medium. In fact, the dynamics of such modulated modes may be described by a nonlinear Schrödinger (NLS) equation, which can be derived from the plasma-hydrodynamic equations using a multiscale perturbation technique (MSPT) [13]. One of the solutions of the NLS equation have an envelope structure called envelope solitons (such as bright envelope soliton and dark envelope soliton) [14, 15]. However, the analysis of modulational instability (MI) of modulated wave packets is the basic rule for studying the formation of bright or dark envelope solitons in the nonlinear medium, like, plasmas medium [16]. Many works have been carried out in the past years to investigate MI and the formation of the electrostatic envelope solitons in many plasma systems. For example, the MI of IAWs in a plasma model composed of positive and negative ions as well as nonthermal electrons has been discussed by Elwakil et al. [17]. They reported that the formation of both dark and bright solitons may be existed in such plasma. The modulated electrostatic wave-packets propagating in a dense electron–positron–ion plasma medium have been examined by McKerr et al. [18]. They obtained that the MI criteria of modulated IAWs are dependence on plasma parameters. Further, Chowdhury et al. [19] have investigated the MI of IAWs in a multi-component plasma system containing inertialess nonextensive electrons-positrons, and heavy negative and light positive ions fluid. Ahmed et al. [20] have examined the MI of IAWs and they found that the critical wavenumber decreases with the increase in the value of wavenumber. Banik at al. [21] have considered a multi-component plasma system containing warm ions fluid, isothermal electrons as well as super-thermal electrons and positrons and examined the MI of IAWs in such plasma system. Recently, Jahan at al. [22] have investigated the criteria of the existence of the envelope structures associated with IAWs in a plasma system having four components, namely, isothermal positrons, nonthermal, nonextensive distributed electrons, and positive-negative ions fluid. They found that the dark and bright envelope solitons can be present in the system.

The aim of the present study is to analyze the conditions for the MI of ion acoustic (IA) wavepackets in a four-component dense plasma system containing positively and negatively charged ion fluids as well as degenerate positrons and electrons. Both positrons and electrons will be considered in the framework of the Thomas-Fermi statistics, while both the negative and positive ions will be treated as a classical fluid. Thus, the plasma system can be modeled by semiclassical hydrodynamics equations. The MSPT will then be used to derive the NLS equation, which describes the nonlinear dynamics of IA wavepackets. Furthermore, the anticipated occurrence of modulated envelope excitations will be discussed in this paper.

The organization of the current paper is as follows; the basic equations are provided in Sect. 2. Using a MSPT, the NLS equation is derived in Sect. 3. The MI analysis of IA wavepackets is given in Sect.4. In Sect. 5, the envelope solitons are discussed. Finally, the conclusions are presented in Sect. 6.

2. Basic equations

Let's consider a multi-component dense plasma system containing negative and positive ions, as well as inertialess degenerate positrons and electrons. Both positive and negative ions are assumed to be as classical fluid, while both positrons and electrons are described by Thomas-Fermi distribution. Hence, the electrons (n_e) and positrons (n_p) densities are respectively given by [23]

$$n_e = n_{e0}\left(1+\frac{e\varphi}{E_{Fe}}\right)^{3/2}, \tag{1}$$

$$n_p = n_{p0}\left(1-\frac{e\varphi}{E_{Fp}}\right)^{3/2}, \tag{2}$$

where $n_{e0}(n_{p0})$ represents the unperturbed electrons (positrons) number density of, φ denotes the electrostatic potential, e is elementary charge. Here,E_{Fj} is the Fermi energy of degenerate electrons $(j=e)$ or degenerate positrons $(j=p)$, which related to the equilibrium number density n_{j0} as

$$E_{Fj} = k_B T_{Fj} = \left(\frac{\hbar^2}{2m}\right)\left(3\pi^2 n_{j0)}\right)^{2/3},$$

where $m = m_e = m_p$ is the mass of electron or positron, $k_B$is Boltzmann's constant and T_{Fj} is Fermi temperature of j−species particle (electrons for$j=e$ and positrons for $j=p$). $\hbar = h/2\pi$, where h refers to the Planck's constant. The dynamics of IAWs in such dense plasma can be described by the following equations

$$\frac{\partial n_+}{\partial t}+\frac{\partial}{\partial x}(n_+ n_+) = 0, \tag{3}$$

$$\frac{\partial u_+}{\partial t}+u_+\frac{\partial u_+}{\partial x} = -\frac{Z_+ e}{m_+}\frac{\partial \varphi}{\partial x}, \tag{4}$$

$$\frac{\partial n_-}{\partial t}+\frac{\partial}{\partial x}(n_-u_-)=0, \quad (4)$$

$$\frac{\partial u_-}{\partial t}+u_-\frac{\partial u_-}{\partial x}=\frac{Z_-e}{m_-}\frac{\partial \varphi}{\partial x}, \quad (5)$$

$$\frac{\partial^2\varphi}{\partial x^2}=\frac{e}{\epsilon_0}\left(n_e+Z_-n_- -n_p-Z_+n_+\right), \quad (6)$$

where $n_+(n_-)$, $u_+(u_-)$, and $m_+(m_-)$ respectively are the number density, fluid velocity and mass of positive (negative) ions. Here, $Z_+(Z_-)$ represents the charge number on the positive (negative) ion and ϵ_0 refers to free space permittivity. For such a plasma, the equilibrium condition reeds $Z_+n_{+0}+n_{p0}=n_{e0}+Z_-n_{-0}$, in which $n_{+0}(n_{-0})$ denotes the unperturbed number density of the positive (negative) ions.

Now, all physical quantities shown in the Eqs. (1)-(7) can be normalized as: $\bar{n}_+=n_+/n_{+0}$, $\bar{n}_-=n_-/n_{-0}$, $\bar{u}_+(\bar{u}_-)=u_+(u_-)/C_+$, and $\phi=e\varphi/E_{Fe}$, where $C_+=\sqrt{E_{Fe}/m_+}$ is the ion acoustic waves speed. The time (t) and space variable (x) are normalized as $\bar{t}=\omega_{pi}t$ and $\bar{\mathrm{x}}=\omega_{pi}\,x/C_+$, respectively where $\omega_{pi}=\sqrt{n_{+0}Z_+^2e^2/\epsilon_0m_+}$ is the plasma frequency of positive ion. Accordingly, we can rewrite the basic equations (1)-(7) in the normalized form:

$$\frac{\partial \bar{n}_+}{\partial \bar{t}}+\frac{\partial}{\partial \bar{x}}(\bar{n}_+\bar{u}_+)=0, \quad (8)$$

$$\frac{\partial \bar{u}_+}{\partial \bar{t}}+u_+\frac{\partial \bar{u}_+}{\partial \bar{x}}=-\frac{\partial \phi}{\partial \bar{x}}, \quad (9)$$

$$\frac{\partial \bar{n}_-}{\partial \bar{t}}+\frac{\partial}{\partial \bar{x}}(\bar{n}_-\bar{u}_-)=0, \quad (10)$$

$$\frac{\partial \bar{u}_-}{\partial \bar{t}}+\bar{u}_-\frac{\partial \bar{u}_-}{\partial \bar{x}}=\mu\frac{\partial \phi}{\partial \bar{x}}, \quad (11)$$

$$\frac{\partial^2\phi}{\partial \bar{x}^2}=\beta\bar{n}_- -\bar{n}_+ +\alpha_e(1+\phi)^{3/2} -\alpha_p(1-\sigma\phi)^{3/2}, \quad (12)$$

where $\mu=Z_-\,m_+/Z_+m_-$ is the mass ratio of positive-to-negative ion, $\alpha_e=n_{e0}/Z_+n_{+0}$, is the number density ratio of electron-to-positive ion,$\alpha_p=n_{p0}/Z_+n_{+0}$ is the number density ratio of positron-to-positive ion, $\beta=Z_-n_{-0}/Z_+n_{+0}$ is the number density ratio of positive-to-negative ion and $\sigma=T_{Fe}/T_{Fp}=f^{2/3}$, $f=n_{e0}/n_{p0}$. We assume that the normalized potential ϕ is small, such that $\phi\ll 1$. Thus, we can expand the functions appearing in the right-hand side of Eq. (12). With that expansion, Eq. (12) simplifies to

$$\frac{\partial^2\phi}{\partial \bar{x}^2}+n_+-\beta n_-=s_0+\,s_1\phi +s_2\phi^2+s_3\phi^3+\cdots, \quad (13)$$

where the term on the right-hand side of the above equation represents the contribution of degenerate electrons and positrons, in which the dimensionless parameters s_0, s_1, s_2 and s_3 are defined as:

$$s_0=\alpha_e-\alpha_p,$$
$$s_1=3(\alpha_e+\sigma\alpha_p)/2,$$
$$s_2=3(\alpha_e-\sigma^2\alpha_p)/8,$$

and

$$s_3=-(\alpha_e+\sigma^3\alpha_p)/16.$$

3. Nonlinear Schrödinger equation

In order to investigate the MI of IA wavepackts in such dense plasma, we go first to derive the NLS equation employing a MSPT. Accordingly, the following stretched space and time variables are considered

$$\xi=\epsilon(\bar{x}-V_g\bar{t}), \qquad \tau=\epsilon^2\bar{t}, \quad (14)$$

where the parameter ϵ is a minor real parameter and V_g reflects the dimensionless group velocity of IA wavepackt, which will be determined later on. The dependent variables i.e.,$\bar{n}_+$, $\bar{n}_-$, $\bar{u}_+$, $\bar{u}_-$ and φ can be expanded as

$$F(\bar{x},\bar{t}) = F_0+\sum_{n=1}^{\infty}\epsilon^n\sum_{l=-n}^{n}F_l^{(n)}(\xi,\tau)\exp(il\Upsilon), \quad (15)$$

were

$$F=[\bar{n}_+,\bar{u}_+,\bar{n}_-,\bar{u}_-,\phi]^T,$$

$$F_l^{(n)}=\left[n_{+l}^{(n)},u_{+l}^{(n)},n_{-l}^{(n)},u_{-l}^{(n)},\phi_l^{(n)}\right]^T,$$

and

$$F_0=[1,0,1,0,0]^T,$$

where $\Upsilon=k\bar{x}-\omega\bar{t}$, k and ω are the real variables representing the wavnumber and angular frequency of the carrier wave, respectively. Since the variables $\bar{n}_+$, $\bar{u}_+$, $\bar{n}_-$, $\bar{u}_-$and ϕ are real, the variables $n_{+l}^{(n)}$, $u_{+l}^{(n)}$, $n_{-l}^{(n)}$, $u_{-l}^{(n)}$ and $\phi_l^{(n)}$ must be satisfy the reality condition $F_l^{(n)}=F_{-l}^{*(n)}$ where the asterisk denotes the complex conjugate. From the Eqs. (14) and (15), the operators $\partial/\partial\bar{t}$ and $\partial/\partial\bar{x}$ appearing in Eqs. (8)-(12) are given as

$$\frac{\partial}{\partial\bar{t}}\to\frac{\partial}{\partial\bar{t}}-\epsilon V_g\frac{\partial}{\partial\xi}+\epsilon^2\frac{\partial}{\partial\tau}, \quad (16a)$$

$$\frac{\partial}{\partial\bar{x}}\to\frac{\partial}{\partial\bar{x}}+\epsilon\frac{\partial}{\partial\xi}. \quad (16b)$$

Inserting the Eqs. (15) and (16) into Eqs. (8)-(13) and collecting the terms in different powers of ϵ parameter. The equations of the first order of $\epsilon(n=1)$ with first order harmonic $(l=1)$ lead to the following relations

$$n_{+1}^{(1)} = \frac{k^2}{\omega^2}\varphi_1^{(1)}, \qquad u_{+1}^{(1)} = \frac{k}{\omega}\varphi_1^{(1)}, \tag{17}$$

$$n_{-1}^{(1)} = -\mu\frac{k^2}{\omega^2}\varphi_1^{(1)}, \quad u_{-1}^{(1)} = -\frac{\mu k}{\omega}\varphi_1^{(1)}, \tag{18}$$

with the following dispersion relation

$$\omega = k\sqrt{\frac{1+\mu\beta}{k^2+s_1}}. \tag{19}$$

Equation (19) indicates the angular frequency ω of IAW is a real quantity, which reflects the stability of the linear waves in the current plasma system. Here, we investigate the effects of plasma parameters on ω.Figure 1(a) depicts the changes of carrier wave frequency ω versus carrier wavenumber k with varying mass ratio of positive-to-negative ion (via μ). It is clear from this figure that the wave frequencyω increases with increasing μ. For large values of k, the wave frequency ω approaches unity. Figures 1(b) and (c) show how the wave frequency ωvarying with wavenumber$k$ for different values of positron concentration, via $\alpha_p\left(=n_{p0}/Z_+n_{+0}\right)$ [Fig. 1(b)], and for different values of the electron concentration, via $\alpha_e(=n_{e0}/Z_+n_{+0})$ [Fig. 1(c)]. We notice from Fig. 1(b) that the wave frequency ω decreases with α_p. The change in ω tend to be weaker for smaller and larger k-value. On the other hand, Fig. 1(c) shows that the wave frequency ω decreases with the increase of the α_e, and the effect is weaker for small values of k.

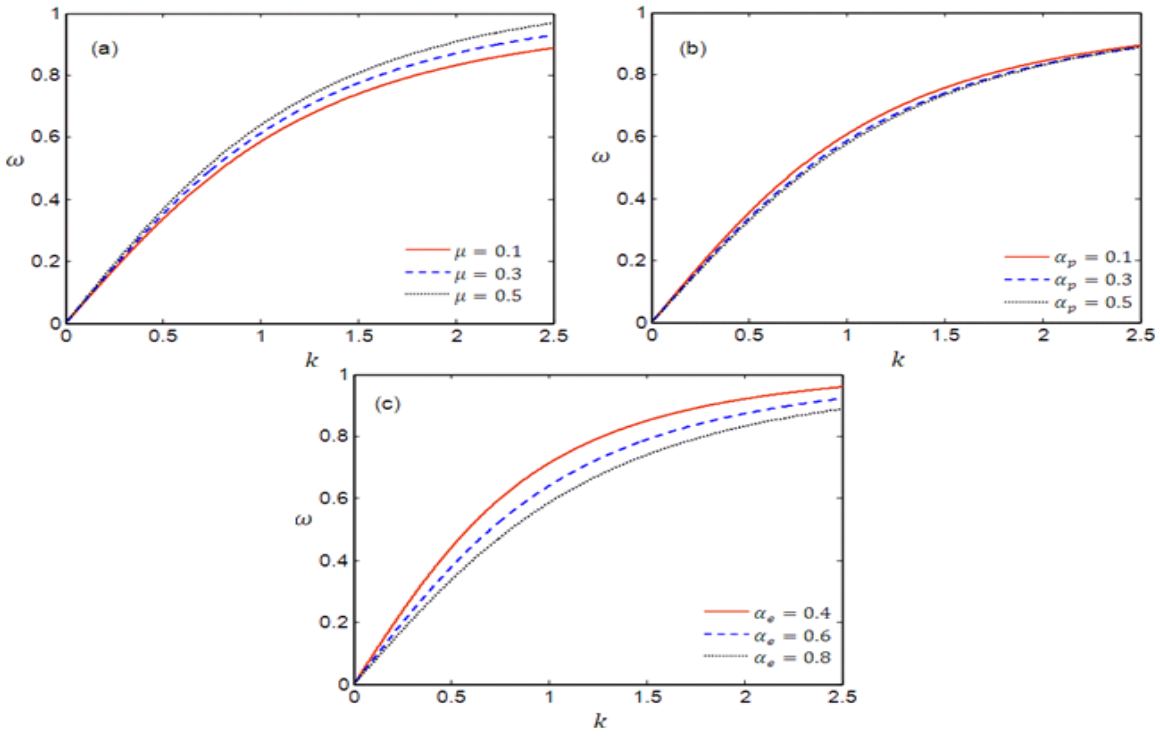

Figure 1: The changes of wave frequency ω versus wavenumber k. (a) plotted for μ different, with $\alpha_e = 0.8$, $\alpha_p = 0.3$; (b) plotted for α_p different, with $\mu = 0.1$, $\alpha_e = 0.8$; and (c) plotted for $\alpha_e$different, for $\mu = 0.1$, and $\alpha_p = 0.3$.

The equations of the second-order in ϵ $(n=2)$ along with the first harmonics $(l=1)$ yields the following relations

$$n_{+1}^{(2)} = \frac{k^2}{\omega^2}\varphi_1^{(2)} + \frac{2ik\left(kV_g-\omega\right)}{\omega^3}\frac{\partial\varphi_1^{(1)}}{\partial\xi}, \tag{20}$$

$$u_{+1}^{(2)} = \frac{k}{\omega}\varphi_1^{(2)} + \frac{i\left(kV_g-\omega\right)}{\omega^2}\frac{\partial\varphi_1^{(1)}}{\partial\xi}, \tag{21}$$

$$n_{-1}^{(2)} = -\frac{\mu k^2}{\omega^2}\varphi_1^{(2)} - \frac{2ik\mu\left(kV_g-\omega\right)}{\omega^3}\frac{\partial\varphi_1^{(1)}}{\partial\xi}, \tag{22}$$

$$u_{-1}^{(2)} = -\frac{\mu k}{\omega}\varphi_1^{(2)} - \frac{i\mu\left(kV_g-\omega\right)}{\omega^2}\frac{\partial\varphi_1^{(1)}}{\partial\xi}, \tag{23}$$

with the following normalized group velocity

$$V_g = \left(\frac{\omega}{k}\right)\left(1 - \frac{\omega^2}{1+\mu\beta}\right). \qquad (24)$$

Figure 2(a) exhibits the dependence of the group velocity (V_g) of IA wavepacket on both wave-number$k$ and mass ratioμ. From the figure, we notice that with an increase in k, the group velocity V_g decreases. As the value of μ increases, the V_g increases as well, and the change turns to be weaker for large k values. Figures 2(b) and 2(c) show the variation of V_g against k for different values of α_p and α_e respectively. It is noted that, the group velocityV_g decreases with the increase in k. For lower values of $k \leq 0.9$, the group velocity V_g decrease with an increment of both α_p and α_e and for larger values of $k > 0.9$, the group velocityV_g turns to increase by increasing α_p or α_e.

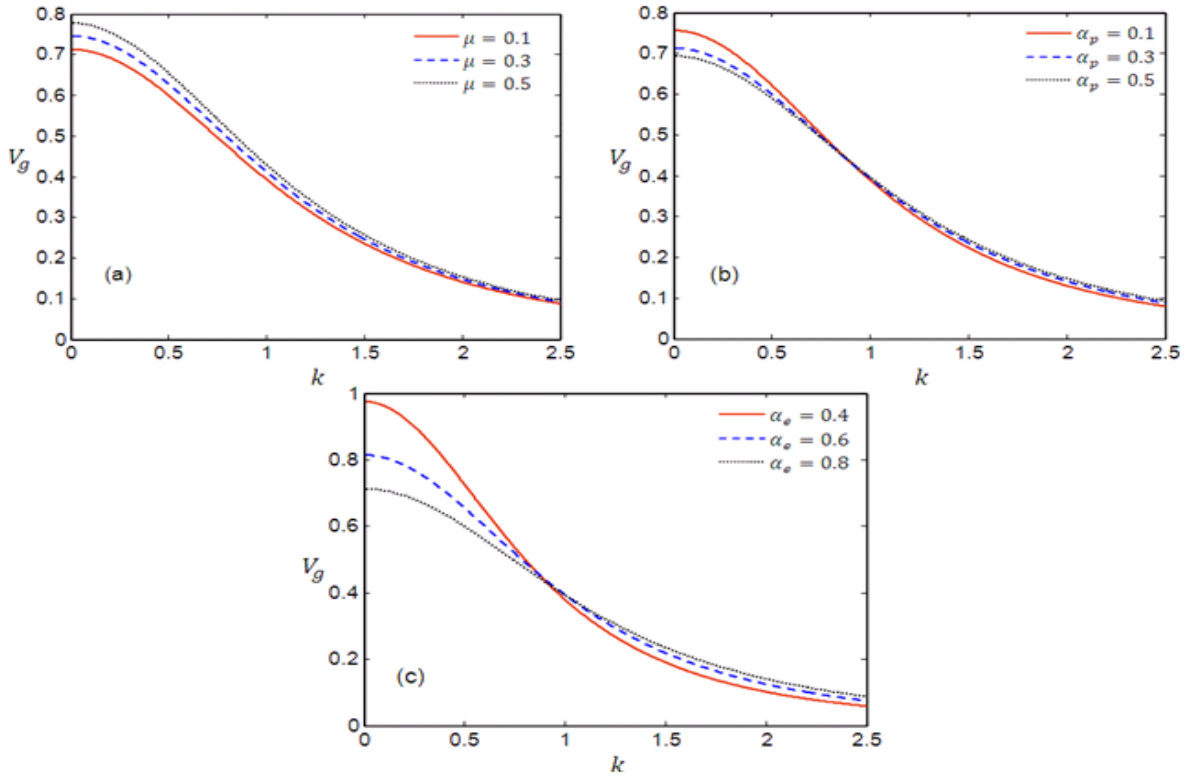

Figure 2: The changes of group velocity V_g versus wavenumber k. (a) plotted for μ different, with $\alpha_e = 0.8, \alpha_p = 0.3$; (b) plotted for α_p different, with $\mu = 0.1, \alpha_e = 0.8$; and (c) plotted for $\alpha_e$different, with $\mu = 0.1$, and $\alpha_e = 0.8$.

From the equations of the second-order $(n = 2)$ with second harmonics $(l = 2)$, we get the expressions of $n_{+2}^{(2)}$, $n_{+2}^{(2)}$, $n_{-2}^{(2)}$, $n_{-2}^{(2)}$ and $\phi_2^{(2)}$ in terms of $\left(\varphi_1^{(1)}\right)^2$ as

$$n_{+2}^{(2)} = C_{+n2}^{(2)}\left(\varphi_1^{(1)}\right)^2, \qquad u_{+2}^{(2)} = C_{+u2}^{(2)}\left(\varphi_1^{(1)}\right)^2, \qquad (25)$$

$$n_{-2}^{(2)} = C_{-n2}^{(2)}\left(\varphi_1^{(1)}\right)^2, \qquad u_{-2}^{(1)} = C_{-u2}^{(2)}\left(\varphi_1^{(1)}\right)^2, \qquad (26)$$

$$\phi_2^{(2)} = C_{\phi 2}^{(2)}\left(\varphi_1^{(1)}\right)^2, \qquad (27)$$

where

$$C_{+n2}^{(2)} = \frac{k^2}{2\omega^4}\left(3k^2 + 2\omega^2 C_{\phi 2}^{(2)}\right),$$

$$C_{+u2}^{(2)} = \frac{k}{2\omega^3}\left(k^2 + 2\omega^2 C_{\phi 2}^{(2)}\right),$$

$$C_{-n2}^{(2)} = \frac{\mu k^2}{2\omega^4}\left(3\mu k^2 - 2\omega^2 C_{\phi 2}^{(2)}\right),$$

$$C_{-u2}^{(2)} = \frac{\mu k}{2\omega^3}\left(\mu k^2 - 2\omega^2 C_{\phi 2}^{(2)}\right),$$

$$C_{\varphi 2}^{(2)} = \frac{3k^4(\mu^2\beta - 1) + 2s_2\omega^4}{2\,\omega^2[k^2(1+\mu\beta - 4\omega^2) - s_1\omega^2]}.$$

From the third-order $(n = 3)$ and second-order $(n = 2)$ equations with zero harmonic $(l = 0)$, the expressions of $n_{+0}^{(2)}$, $n_{+0}^{(2)}$, $n_{-0}^{(2)}$, $n_{-0}^{(2)}$ and $\phi_0^{(2)}$ are obtained in terms of $\left|\varphi_1^{(1)}\right|^2 = \varphi_1^{(1)}\varphi_1^{*(1)}$ as

$$n_{+0}^{(2)} = C_{+n0}^{(2)}\left|\varphi_1^{(1)}\right|^2, \qquad u_{+0}^{(2)} = C_{+u0}^{(2)}\left|\varphi_1^{(1)}\right|^2, \qquad (28)$$

$$n_{-0}^{(2)} = C_{-n0}^{(2)} \left|\varphi_1^{(1)}\right|^2, \quad u_{-0}^{(1)} = C_{-u0}^{(2)} \left|\varphi_1^{(1)}\right|^2, \quad (29)$$

$$\phi_0^{(2)} = C_{\phi 0}^{(2)} \left|\varphi_1^{(1)}\right|^2, \quad (30)$$

where

$$C_{+n0}^{(2)} = \frac{k^2\left(\omega + 2kV_g\right) + \omega^3 C_{\phi 0}^{(2)}}{V_g^2 \omega^3},$$

$$C_{+u0}^{(2)} = \frac{\omega^2 C_{\phi 0}^{(2)} + k^2}{V_g \omega^2},$$

$$C_{-n0}^{(2)} = \frac{\mu^2 k^2\left(\omega + 2kV_g\right) - \mu\omega^3 C_{\phi 0}^{(2)}}{\omega^3 V_g^2},$$

$$C_{-u0}^{(2)} = \frac{\mu^2 k^2 - \mu\omega^2 C_{\phi 0}^{(2)}}{\omega^2 V_g},$$

$$C_{\varphi 0}^{(2)} = \frac{k^2\left(\omega + 2k\, V_g\right)(\mu^2\beta - 1) + 2s_2 V_g^2 \omega^3}{\omega^3\left(1 + \mu\beta - s_1 V_g^2\right)}.$$

Finally, using the Eqs. (17)-(30) into the third-order ($n = 3$) equations with first harmonic ($l = 1$), we obtain the following NLS equation:

$$i\frac{\partial \Phi}{\partial \tau} + P\frac{\partial^2 \Phi}{\partial \xi^2} + Q|\Phi|^2\Phi = 0, \quad (31)$$

where we set $\Phi = \phi_1^{(1)}$ for simplicity. The nonlinear coefficient Q is deduced to be

$$\begin{aligned} Q = \frac{\omega^3}{2k^2(\beta\mu + 1)}\Bigg[& 2\, s_2\left(C_{\varphi 2}^{(2)} + C_{\varphi 0}^{(2)}\right) \\ & - \frac{2\, k^3}{\omega^3}\left(C_{+u2}^{(2)} + C_{+u0}^{(2)}\right) \\ & - \frac{k^2}{\omega^2}\left(C_{+n0}^{(2)} + C_{+n2}^{(2)}\right) \\ & - \frac{2\beta\mu k^3}{\omega^3}\left(C_{-u0}^{(2)} + C_{-u2}^{(2)}\right) \\ & - \frac{\beta\mu k^2}{\omega^2}\left(C_{-n0}^{(2)} + C_{-n2}^{(2)}\right) \\ & + 3s_3\Bigg], \end{aligned} \quad (32)$$

while the dispersion coefficient P given as

$$P = \frac{3V_g(kV_g - \omega)}{2\omega k}. \quad (33)$$

4. Analysis of modulational instability

To Investigate the MI of IA wavepackets, we consider the following harmonic wave solution of NLS equation (31) [12]

$$\Phi = \tilde{\varphi}\exp(iQ\varphi_0^2\tau) \quad (31)$$

where $\tilde{\varphi} = \varphi_0 + \varphi_1$ withφ_0 is a real constant amplitude and φ_1 is a small perturbation amplitude where $|\varphi_1| \ll \varphi_0$. Now, using Eq. (34) into Eq. (31) and linearizing we get the following equation

$$i\frac{\partial \varphi_1}{\partial \tau} + P\frac{\partial^2 \varphi_1}{\partial \xi^2} + Q\varphi_0^2(\varphi_1 + \varphi_1^*) = 0, \quad (35)$$

where φ_1^* denotes the complex conjugate of φ_1. Now, we consider the solution of Eq. (35) in the form

$$\varphi_1(\xi,\tau) = [F(\xi,\tau) + iG(\xi,\tau)]\exp(i\Psi), \quad (36)$$

where $\Psi = \mathrm{K}\xi - \Omega\tau$ is the modulation phase with K and Ωare respectively the modulation wavenumber and the modulation frequency of IA wavepackets. Inserting this solution into Eq. (35), and separating the imaginary and real parts, we get two coupled equations, which allow taking the following matrix form

$$\begin{pmatrix} i\Omega & P\mathrm{K}^2 \\ 2Q\phi_0^2 - P\mathrm{K}^2 & i\Omega \end{pmatrix}\begin{pmatrix} F \\ G \end{pmatrix} = \begin{pmatrix} 0 \\ 0 \end{pmatrix}. \quad (37)$$

Clearly, the determinant of the above matrix must be zero, which leads to the following dispersion relation

$$\Omega^2 = \mathrm{K}^4\left(P^2 - 2PQ\frac{\phi_0^2}{\mathrm{K}^2}\right). \quad (38)$$

Equation (38) is the modulated dispersion relation for IA wavepackets. As it's noted from Eq. (38) thatthe modulated IA wavepackets will be stable for all values of K when the PQ product is negative value(i.e., when $PQ < 0$). On the other hand, when the PQ product is positive value, the instability occurs in the region in which the values of the modulational wavenumber K are below a critical value $\mathrm{K}_{cr} = \phi_0\sqrt{2\,Q/P}$. Otherwise, when $PQ = 0$, there is a critical value of carrier wavenumber $k(= k_{cr})$ separating stable ($PQ < 0$), and unstable ($PQ > 0$) regions for IA wavepackets.Therefore, we will investigate how the critical wavenumber k_{cr} depends on the plasma parameters (i.e., μ, α_e and α_p). Figure 3 shows the contour plot of the PQ product, in the space (μ, k). Clearly, this figure indicates that the value of the critical wavenumber k_{cr} decreases as μincreases. This means that the instability region shifts to lower wavenumber as the values of μ

increases.The dependence of k_{cr}on the electrons and positrons concentrations (via the parameters α_e andα_p) are depicted in the Figs. 4 and 5 respectively.

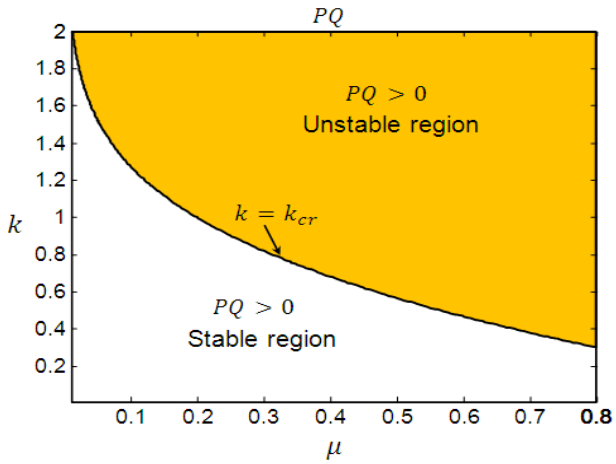

Figure 3: Contour plot of PQ product is depicted against k andμ, along with $\alpha_p = 0.3$, and $\alpha_e = 0.7$.

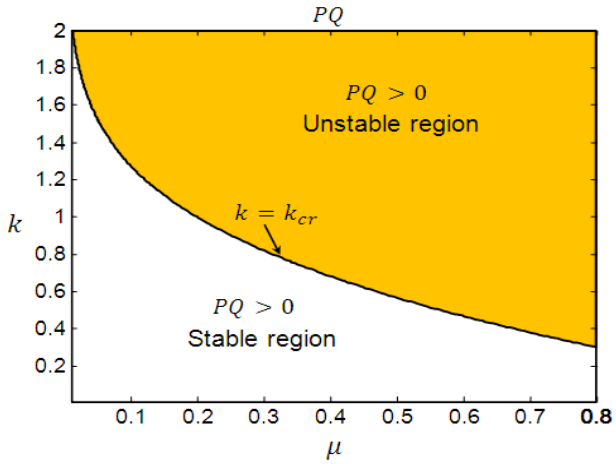

Figure 4: Contour plot of PQ product is depicted k and α_e, along with $\mu = 0.5$ and $\alpha_p = 0.3$.

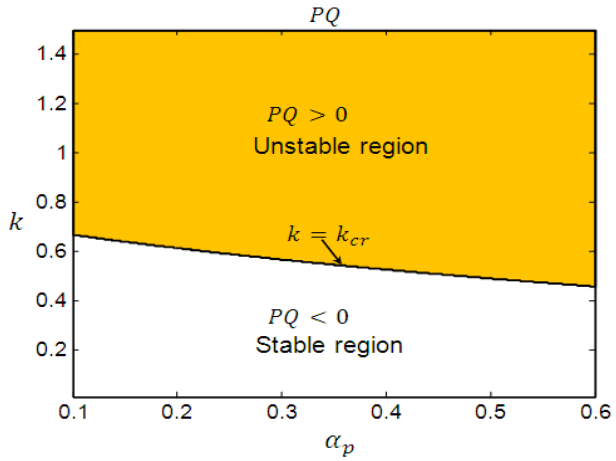

Figure 5: Contour plot of PQ product is depicted against k and α_p, along with $\mu = 0.5$, and $\alpha_e = 0.7$.

One can notice from Fig. 4 that the effect of electrons concentration$\alpha_e$is to narrow the wavenumber domain for the onset of instability i.e., the stability region shifts to higher wavenumber with the increase of α_e.As a result of the increase in the value of α_p, the value of the critical wavenumber k_{cr}decreases (see Fig. 5). This means that at the higher values of α_p, the instability domain occurred at lower values of carrier wavenumber k.

Furthermore, in the unstable region, the modulational instability growth rate (MIGR) of the IA wavepackets can be obtained from Eq. (38) in the form

$$\eta_g = |P|K^2\sqrt{K_{cr}^2/K^2 - 1}. \qquad (39)$$

Lt's noticed that, for$K = K_{cr}/\sqrt{2}$, the MIG has a maximum value η_{gm}, given as $\eta_{gm} = |Q|\phi_0^2$. Figures 6 and 7 show how the MIGR$\eta_g$changes with the modulational wavenumber K for different values of μ and α_p, respectively. It's found from Figs. 6 and 7 that the magnitudes of MIGR (η_g) are larger for the larger values of μ and α_p. Also, is to enlarge the maximum value of η_g.

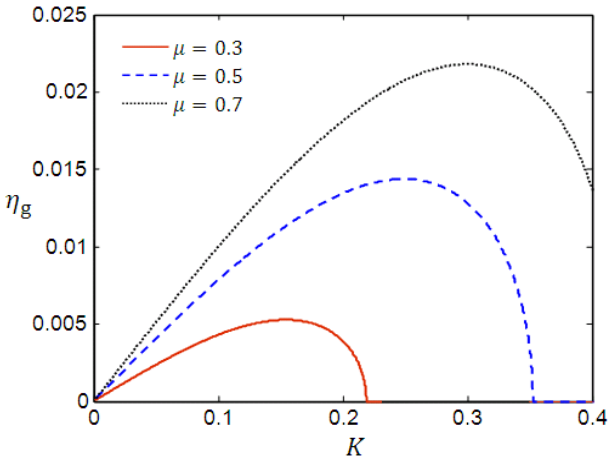

Figure 6: The variation of MIGR (η_g) against K for different values of μ with $\alpha_e = 0.7$, and $\alpha_p = 0.3$.

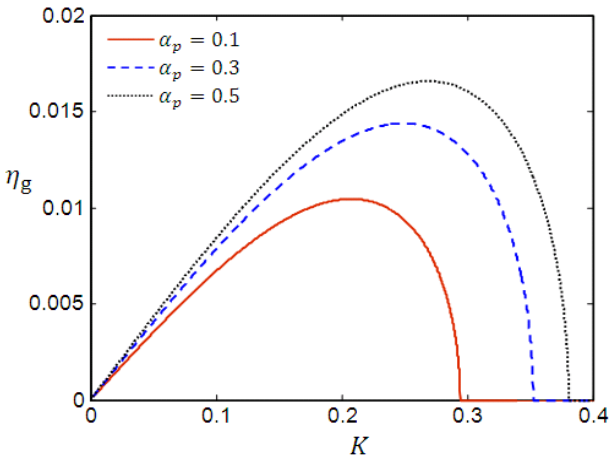

Figure 7: The variation of MIGR (η_g) against K for different values of α_p with $\alpha_e = 0.7$, and $\mu = 0.5$.

5. Envelope IA solitons

Generally, the NLS equation (31) can have space-localized solutions of envelope-soliton type, which may be arisen due to the effects of nonlinearity and dispersion. Focusing on two types of envelope solitons may be existed in the current plasma system, namely, bright-type envelope solitons (pulse) and dark-type envelope solitons (holes), depending on the sign of the PQ product. The expressions for envelope solitons can be found by setting the space-localized solutions of Eq. (31) on the form [14]

$$\Phi(\xi,\tau) = \sqrt{\psi(\xi,\tau)}\ \exp\left[\frac{i}{2P}\Theta(\xi,\tau)\right], \qquad (40)$$

where$\psi(\xi,\tau)$ reflects the envelope profile and $\Theta(\xi,\tau)$ represents the nonlinear phase shift whose expressions can be determined by inserting the above equation into Eq. (31)depending on the sign of the PQ product.

5.1 Bright envelope solitons

If thePQ product is positive value, the solution (40) correspond to bright envelope soliton (or bright pulse), in which the envelope form ψ and nonlinear phase shift Θ are given by [14]

$$\psi = \psi_0 \operatorname{sech}^2\left(\frac{\xi - U\tau}{L}\right),$$
$$\Theta = U\xi - \left(\Omega_0 + \frac{U^2}{2}\right)\tau, \qquad (41)$$

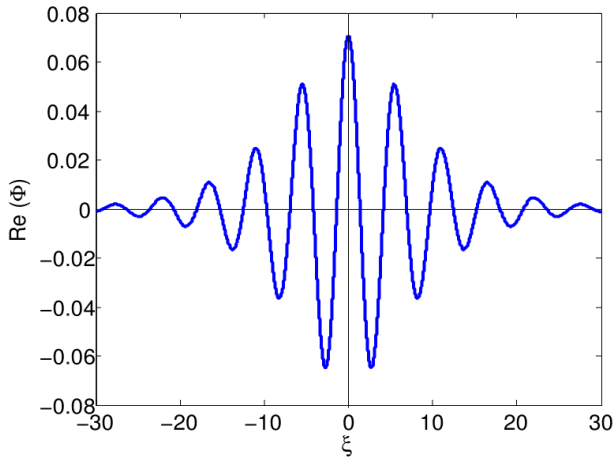

Figure 8: The profile of the bright envelop soliton at $\tau = 0$ with $\alpha_e = 0.7, \alpha_p = 0.3, \mu = 0.3, \psi_0 = 0.005\,, k = 1, \Omega_0 = 0.25$, and $U = 0.5$

where ψ_0 indicates the pulse amplitude, Ω_0 is the oscillating frequency at rest, U is the travelling speed of the localized pulse and L is pulse width. It should be mentioned here that the pulse width L is proportional to the maximumamplitude of bright soliton $\sqrt{\psi_0}$, that can be written as$L = \sqrt{2P/Q\psi_0}$. For positive values ofPQ-product, the MI of the IAWs associated with unstable domain leads to generate a bright pulse with fast oscillations inside the packet as shown in Fig. 8. As can be seen from the Fig. 8, when $\xi = 0$, the pulse height is maximum value, and decreases with an increase of the positive or negative values of ξ. When $\xi \to \pm\infty$, the pulse tends to zero. Additionally, Fig.9shows the time evolution of the bright envelope soliton, while the Fig. 10 shows the bright envelope soliton pulse for different values ofμ. As shown from Fig. 10, the pulse width decreases with the increase of μ.

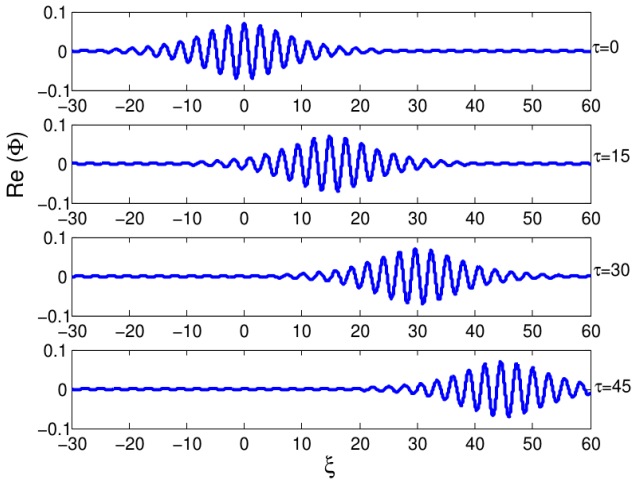

Figure 9: The profiles of the bright envelop solitons at successive times with $U = 1$. The other parameters are the same as in Fig. 8.

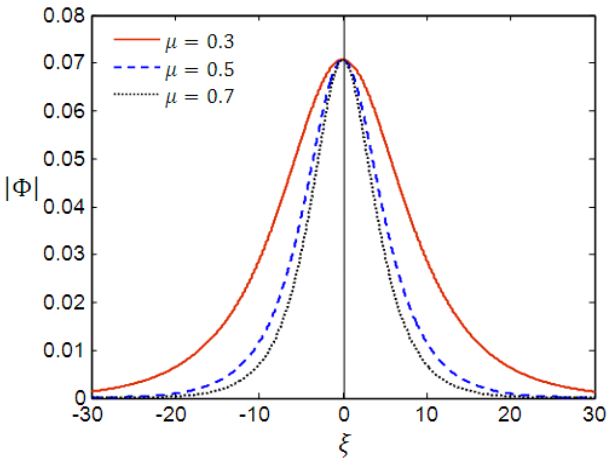

Figure 10: The variation of $|\Phi|$ versus ξ, for μ different when $PQ > 0$, and with$\alpha_e = 0.7, \alpha_p = 0.3\,, \mu = 0.3, \psi_0 = 0.005\,, k = 1, \Omega_0 = 0.25$, and $U = 0.5$.

5.2 Dark envelope solitons

The dark envelope solitons (or dark pulses) can be formed in the system when the values of PQ productare negative ($PQ < 0$). In this case the real functionsψ, and Θ are given by [14]

$$\psi = \psi_1 \tanh^2\left(\frac{\xi - U\tau}{L_1}\right),$$
$$\Theta = U\xi + \left(2PQ\psi_1 - \frac{U^2}{2}\right)\tau, \qquad (42)$$

where the dark pulse width L_1 depends on the maximum amplitude$\sqrt{\psi_1}$ via $L_1 = \sqrt{2|P/Q\psi_1|}$.

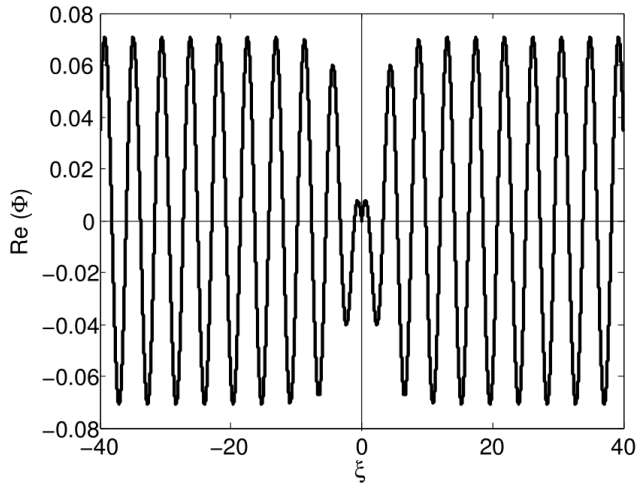

Figure 11: The profile of the dark envelope soliton at $\tau = 0$ with $\alpha_e = 0.7$, $\alpha_p = 0.3$, $\mu = 0.3$, $\psi_1 = 0.005$, $k = 0.3$, and $U = 0.5$.

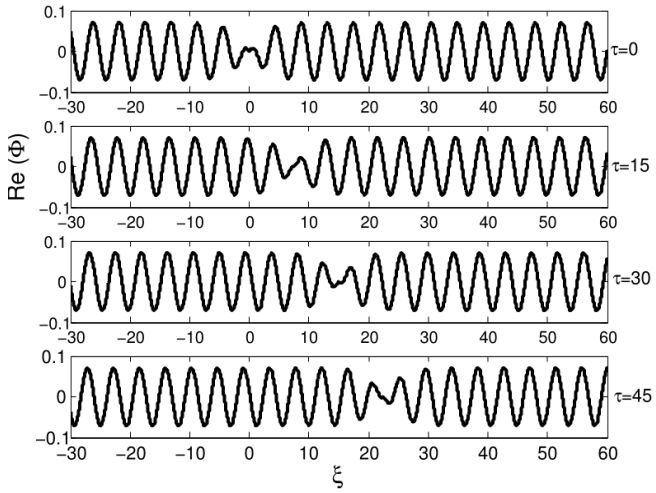

Figure 12: The profiles of the dark envelope solitons at successive times with $U = 1$. The other parameters are the same as in Fig. 11.

The profile of the dark envelope soliton with $\tau = 0$, and $k = 0.3$ can be observed in Fig. 11. It's noted that the propagation of dark envelope soliton is corresponded to a propagating a void (hole) amidst a constant region where we notice that $|\Phi|$ decreases from a finite value at infinity and then returns to its state. Addition, the time evolution of dark envelope soliton is shown in Fig. 12. Further, Fig. 13 shows how the width of the dark envelope solitons is influenced by mass ratio μ. From Fig. 13 one can, be see that the width of dark envelope soliton increases with the increase of μ.

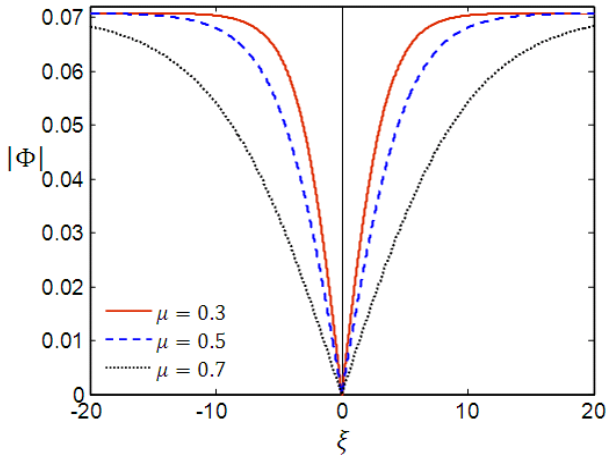

Figure 13: The variation of $|\Phi|$ versus ξ for μ different, when $PQ < 0$, and with $\alpha_e = 0.7$, $\alpha_p = 0.3$, $\psi_1 = 0.005$, $k = 0.3$ and $U = 0.5$.

6. Conclusions

In this paper, the modulated IA wavepackets are investigated in a multicomponent dense plasma model containing inertialless degenerate electrons and positrons as well as negative and positive ions. The electrons and positrons have been considered to be follow Thomas–Fermi distribution, while the ions (positive or negative) were assumed to be inertial and cold. The NLS equation is derived employing a MSPT. Both the modulationally stable and unstable domains can be observed in this model. The effects of dense plasma parameters, i.e., the electrons concentration (α_e), positrons concentration (α_p) and mass ratio of positive-to-negative ion (μ) on the conditions for the modulational instability to occur are discussed. It's found that the instability domains for the wave packets are significantly changed by these parameters. The analysis also shows that the value of MIGR (η_g) decreases with increases of both μ and α_p for fixed other parameters. Moreover, the expressions of the bright and dark envelope solitons are obtained. It's found that the width of the bright (dark) envelope solitons decreases (increases) with the increase in the mass ratio (μ), while their amplitudes remain unchanged. Finally, we expect that our results may be useful for understanding the nonlinear phenomena in compact astrophysical objects as well as in dense plasmas resulting from ultra-intense laser pulses.

References

[1] SHAPIRO, S. L.; TEUKOLSKY, S. A. *Black Holes: White Dwarfs and Neutron Stars: The Physics of Compact Object*.1st Edition, Wiley, NewYork,1983, https://doi.org/10.1002/9783527617661

[2] JUNG, Y. D. *Quantum mechanical effects on electron-electron scattering in dense high temperature plasmas*. Phys. Plasmas 8, (2001) 3842,doi:10.1063/1.1386430

[3] MALKIN, V. M.; FISCH, N. J.; WURTELE, J. S. *Compression of powerful x-ray pulses to at to second durations by stimulated Raman backscattering in plasma*. Phys. Rev. E 75, (2007) 026404, doi:10.1103/PhysRevE.75.0

[4] MARKOWICH, P. A.; RINGHOFER, C.A.; SCHMEISER, C. *Semiconductor Equations* Springer-Verlag, New York, 1990, https://doi.org/10.1007/978-3-7091-6961-2

[5] MEREROVICH, B. E. *High-Current Channel. FIMA*. Moscow, 1999.

[6] ABDELSALAM, U. M.; ALI, S.; KOURAKIS, I. *Nonlinear electrostatic excitations of charged dust in degenerate ultra-dense quantum dusty plasmas*. Phys. Plasmas 19, (2012) 062107, https://doi.org/10.1063/1.4729661

[7] IRFAN, M.; ALI, S.; MIRZA, A. M. *Dust-acoustic solitary and rogue waves in a Thomas-Fermi degenerate dusty plasma*. Astrophys. Space Sci. 353, (2014) 515, https://doi.org/10.1007/s10509-014-2079-4

[8] GIRIFALCO, L. A. *Statistical Physics of Materials*. 1nd Edition, John Wiley & Sons, New York, 1973, p 346

[9] DUBINOV, A. E.; DUBINOVA, A. A. *Nonlinear theory of ion-acoustic waves in an ideal plasma with degenerate electrons.* Plasma Phys. Rep. 33, (2007) 859-870, https://doi.org/10.1134/S1063780X07100078

[10] ABDELSALAM, U. M.; MOSLEM, W. M.; SHUKLA, P. K. *Ion-acoustic solitary waves in a dense pair-ion plasma containing degenerate electrons and positrons*. Phys. Lett. A 372, (2008) 4057–4061, https://dx.doi.org/10.1016/j.physleta.2008.02.086

[11] MEHDIOOR, M.; ESFANDYARI-KALEJAHI, A. *Higher-order corrections to ion acoustic waves in degenerate electron-positron-ion plasmas.*Astrophys. Space Sci. 342, (2012) 93–104, https://doi.org/10.1007/s10509-012-1152-0

[12] KHALED, M. A. H.; SHUKRI, M. A.; AL-SHAIBANI, A. A. *Modulational instability of dust acoustic waves in an opposite polarity dusty plasma in the presence of generalized polarization force with superthermal electrons and Ions*. Braz. J. Phys. 51, (2021) 1290-1302, https://doi.org/10.1007/s13538-021-00920-9

[13] TANIUTI, T.; YAJIMA, N. J. *Perturbation method for a nonlinear wave modulation. I.* J. Math. Phys. 10, (1969) 1369-1372, https://doi.org/10.1063/1.1664975

[14] KOURAKIS, I.; SHUKLA, P. K. *Exact theory for localized envelope modulated electrostatic wavepackets in space and dusty plasmas*. Nonlinear Process Geophys. 12, (2005) 407-423, https://doi.org/10.5194/npg-12-407-2005

[16] RAPTI, Z.; KEVREKIDIS, P. G.; SMERZI, A.; BISHOP, A. R. *Variational approach to the modulational instability.* Phys. Rev. E 69, (2004) 017601, https://doi.org/10.1103/PhysRevE.69.0

[17] El-WAKIL, S. A.; El-SHEWY, E. K.; ABDEL-WAHED, H. G. *Envelope ion-acoustic solitary waves in a plasma with positive-negative ions and nonthermal electrons*. Phys. Plasmas 17, (2010) 052301, https://doi.org/10.1063/1.3383052

[18] MCKERR, M.; KOURAKIS, I.; HAAS, F. *Freak waves and electrostatic wavepacket modulation in a quantum electron–positron–ion plasma*. Plasma Phys. Control. Fusion 56, (2014) 035007, https://doi.org/10.1088/0741-3335/56/3/035007

[19] CHOWDHURY, N. A.; MANNAN, A.; HASAN, M. M.; MAMUN, A. A. *Heavy ion-acoustic rogue waves in electron-positron multi-ion plasmas*. Chaos 27, (2017) 093105, https://doi.org/10.1063/1.4985113

[20] AHMED, N.; MANNAN, A.; CHOWDHURY, N. A.; MAMUN, A. A. *Electrostatic rogue waves in double pair plasmas*. Chaos 28, (2018) 123107doi:10.1063/1.5061800

[21] BANIK, S.; HEERA, N. M.; YEASHNA, T.; HASSAN, Md. R.; SHIKHA, R. K.; CHOWDHURY, N. A.; MANNAN, A.; MAMUN, A. A. *Modulational instability of ion-acoustic waves and associated envelope Solitons in a multi-component plasma*. Gases 1**,** (2021) 148–155, https://doi.org/10.3390/gases1030012

[22] JAHAN, S.; SHIKHA, R. K.; MANNAN, A.; MAMUN, A. A. *Modulational instability of ion-acoustic waves in pair-ion plasma*. Plasma 5, (2022) 1–11, https://doi.org/10.3390/plasma5010001

[23] El-SHAMY, E. F.; MOSLEM, W. M.; SHUKLA, P. K. *Head-on collision of ion-acoustic solitary waves in a Thomas-Fermi plasma containing degenerate electrons and positrons*. Phys. Lett. A 374, (2009) 290–293, https://doi.org/10.1016/j.physleta.2009.10.060